A Novel, Shooting and Bouncing Rays Technique for Propagation Prediction, Based on a Varying-Step Calculation Procedure

Antonis G. Dimitriou, *Student Member IEEE*, and George D. Sergiadis, *Member, IEEE*

***Abstract*—As site specific propagation modeling has become crucial for most modern wireless systems' applications, running-time of the corresponding "ray tracing" techniques is a key issue. We propose a new shooting and bouncing rays (SBR) technique that optimizes the performance of traditional SBR methods in terms of running time, for the same accuracy requirements. This is accomplished via shooting rays towards the quadrangularly arranged locations of interest and performing the calculations at specific distance-intervals. The proposed method is straightforward and can be easily implemented in a ray tracing propagation prediction tool. The main computational advantage, compared to the traditional approaches, results from not performing the reception-sphere tests. The proposed SBR technique is thoroughly explained and the corresponding advantages are demonstrated.**

***Index Terms*—Geometrical Optics, Ray tracing, Electromagnetic propagation,**

I. Introduction

THE great penetration of modern wireless systems, combined with the constant trend for increasing data rates have led to cell shrinking, in the case of traditional cellular networks. This is accomplished, by placing the transmitting antennas well below rooftop level, as mirrored in the planning philosophy of 3G systems. Concurrently, WLAN solutions are widely adopted. In such cases, where propagation strongly depends on the specific environment, deterministic propagation-prediction models based on a combination of geometrical optics and the uniform theory of diffraction, [1]—[11], represent the unique solution for acquiring reliable estimations.

The properties that characterize the performance of such models are accuracy and running-time. The latter is particularly important for most applications, e.g. network planning, where one might repeat a simulation several times for different antenna configurations, so as to decide on the final installation. Naturally, the efforts after the early 90s, [5]—[11], focus on accelerating the performance of the early techniques. For a complete list of all relevant reports, one should refer to [12]—[14].

The authors are with the Aristotle University of Thessaloniki, School of Engineering, Dept. of Electrical & Computer Engineering, Telecommunications Laboratory, Thessaloniki, Greece – GR-54124 (email: sergiadi@auth.gr) (email:antodimi@mri.ee.auth.gr).

In terms of the philosophy of the ray-tracing procedure, two major categories of methods can be distinguished; those based on the image concept, [1]—[2], [7]—[8], and the shooting and bouncing rays (SBR) techniques, [3]—[6].

According to the SBR technique, rays are launched from the transmitter towards all directions, splitting the area in almost constant solid angles. Each ray is traced and when it crosses an obstacle, it is split in a transmitted and a reflected one. Wedges, edges or other discontinuities are treated as 2^{ndary} sources of radiation, by appropriately calculating diffraction.

The main drawback of these techniques arises from the mismatch between the geometry of the study grid and that of the shooting technique, as represented in Fig. 1. Rays are launched from the source, considered to be the center of a sphere, in almost equal solid angles, so as to cover all the region of interest, while the calculation points are usually arranged in an orthogonal grid. As a consequence, the sought resolution at the extremes of the region of interest results in unnecessary high ray-density around the calculation points at the area near the source (over-resolution).

In order to ensure that for each actual path, a single ray is included in the calculations, a reception sphere of radius $R = ad/\sqrt{3}$ that depends on the total distance d traveled by a ray and its angular separation a with the neighboring ones is considered around each receiver's location [3]—[4]. Only the ray that crosses the sphere is considered to have reached the specific location. Since this control is repeated for all rays and the corresponding calculation points, it degrades the performance of the technique, by greatly increasing the total running-time.

We propose a new way of shooting rays and calculating their effects in the study area that surmounts this disadvantage of the classic SBR techniques. Instead of considering rays uniformly arranged, inside a sphere, we consider only these rays that target the quadrangularly arranged study points in the area of interest, as shown in Fig. 3. We therefore avoid the useless calculations. This is accomplished by adopting a varying step calculation procedure. The algorithm guarantees optimum performance of the SBR method in terms of running-time while preserving the same accuracy.

The proposed shooting concept is explained in section II. The entire algorithm is described analytically in section III. In

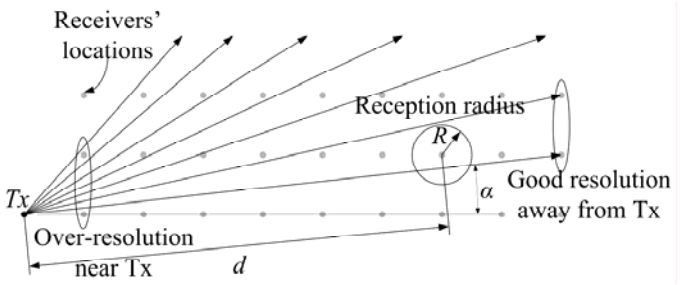

Fig. 1. Representation of the classic SBR approach

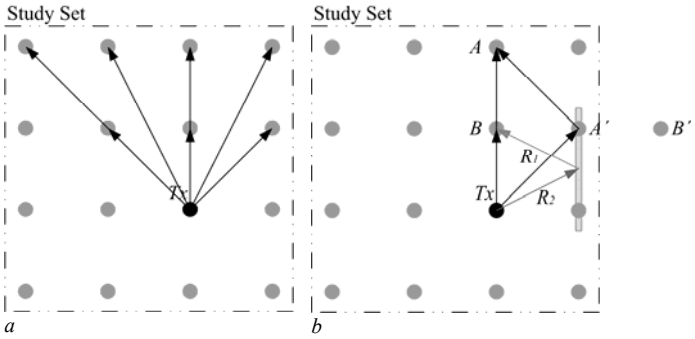

Fig. 2. a) Direct calculation of the field's values at the points of interest. b) Calculation-failure of the reflected ray at point B.

section IV, the proposed method is compared theoretically with the classic SBR approach. Some typical results are presented in section V and we conclude in section VI.

II. Proposed Shooting Technique

A. Description of the Shooting Technique

Let's consider a quadrangularly arranged set of points around the transmitting antenna and assume that calculations, regarding the received E/M field's characteristics must be performed at these locations, as shown in Fig. 2a. We name this set of points as "Study set". Since we are interested in calculating the field's values at these points, let's consider all the rays that initiate from the antenna *Tx* and target the points of the "Study set". This procedure would be sufficient to calculate the field's strength in an "obstacle-free" area. When an obstacle is considered, as shown in Fig. 2b, a new path, through reflection, exists for certain points of the "Study set". Such a path would cross point A, since point A′ is targeted, but reflection at point B would not be considered, unless point B′, outside the "Study set", is targeted.

This problem can be resolved by considering new rays, targeting points outside the study set. To maintain the same resolution in the space surrounding the transmitter, the set of targeted points should form a cube centered at the source.

In the proposed SBR technique, we consider a superset of the "Study set", the "Targeting set" that forms a cube centered at the transmitter. Shooting in the study area is performed by considering all rays emanating from the transmitting antenna towards all the points of the "Targeting set".

The characteristics of the propagating electromagnetic wave along each ray are calculated every integer multiple of the

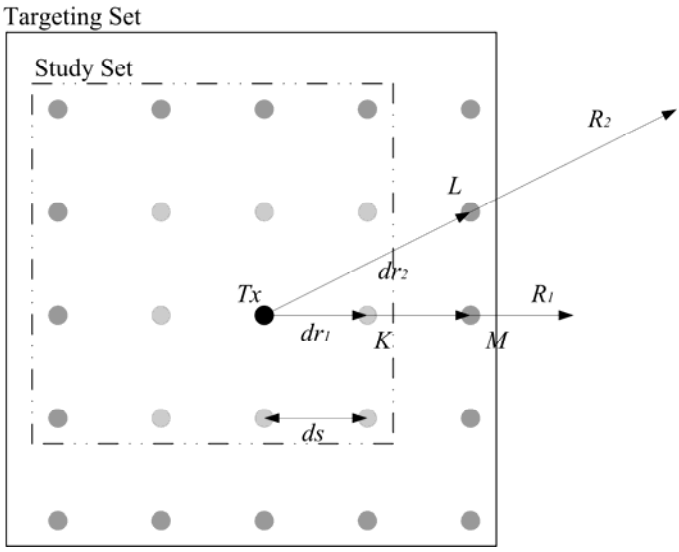

Fig. 3. Representation of the proposed SBR technique.

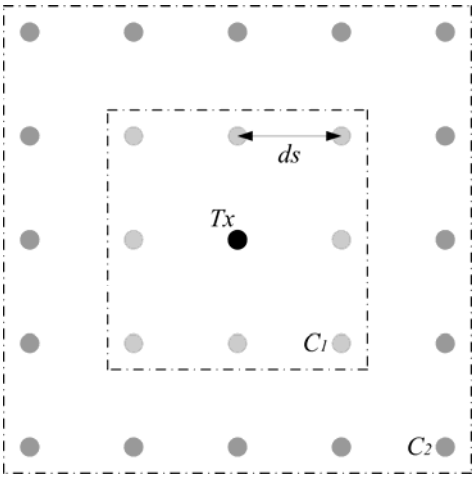

Fig. 4. Ray launching is carried out towards the outer cubes.

initial distance dr_i, as explained in Fig. 3. For each generated ray, dr_i equals the distance from the antenna to the 1st target-point. For example, for the ray R_1, that targets point *K*, the calculations take place every integer multiple of $dr_1 = \left|\overrightarrow{OK}\right|$. As for point *L*, calculations across ray R_2 are carried out every $dr_2 = \left|\overrightarrow{OL}\right|$.

No reception-sphere test is needed to ensure that a single ray is considered for each actual ray path. Since the objects are randomly arranged in the study area, after an incidence, the calculation-points will not necessarily coincide with a study point. In such a case, the field's characteristics are stored at the nearest study point.

We divide the "Targeting set" into subsets C_i, by forming cubes centered at the field's source, as shown in Fig. 4. Each set C_i contains the points that belong to the surface of the corresponding cube. Ray launching occurs from the inner cubes towards the outer. It can be easily proven that:

Each ray that originates from the antenna and targets a point that belongs to C_i will also target one point that belongs to C_j,

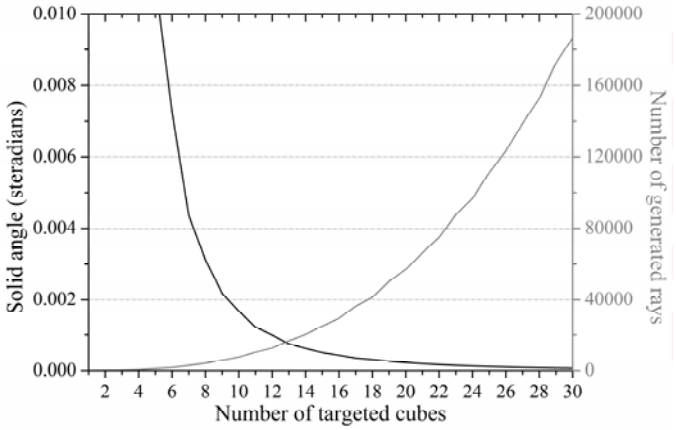

Fig. 5. Variation of the resolution at increasing number of rays.

with, $j > i$, if and only if $j=ki$, $k \in \mathbb{N}_+^* - \{1\}$.

For example, point *M* of Fig. 3 that belongs to C_2, is targeted by R_1, initiated from set C_1. Hence, no new ray is to be launched for that point.

Diffraction points are treated as secondary sources of radiation and the same shooting procedure is carried out around them. Since such points are not necessarily part of the initial "Targeting set", a new set is considered around them and the calculations at each position are stored to the nearest point of the "Study set".

B. Selecting the Spacing of the "Targeting Set"

The spacing of the "Targeting set" is determined by the desired spacing among neighboring points of the "Study set". The latter is typically chosen according to the size and the spacing among objects in the propagation area. For indoor environments, where small objects are usually considered, typical values of *ds* range from 1m to 5m, whereas for small outdoor microcells, where large exterior walls are considered, it ranges from 5m to 20m.

C. Size of the "Targeting Set"

The size of the "Targeting set" is selected based on the desired angular resolution in the propagation area. This can be chosen by setting the desired maximum distance among two neighboring rays, launched from the transmitter, at the boundaries of the propagation area. The graph in Fig. 5 represents the resolution in steradians at increasing targeting cube C_i and the related number of generated rays, assuming the approximation that the departing rays divide space into equal solid angles. Hence, the corresponding solid angle is given as:

$$\Omega = 4\pi / N \quad (1)$$

where *N* is the total number of rays launched from the transmitting antenna.

D. Advantages of the Proposed Shooting Concept

In order to demonstrate the advantages of the proposed shooting technique, we will compare it with the classic SBR approach for the same resolution requirements.

Let's consider an unobstructed area and assume that we wish to calculate the received field strength at point *Rx* of Fig.

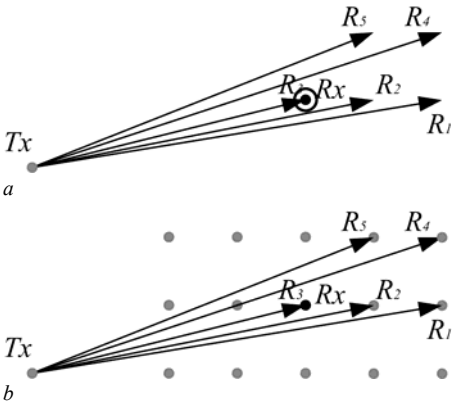

Fig. 6. Comparison of the proposed technique with the classic SBR at free space

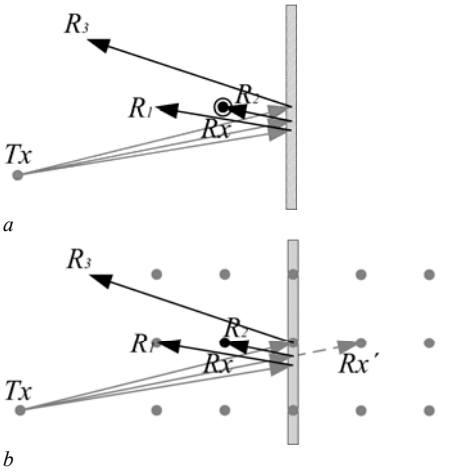

Fig. 7. Comparison of the proposed technique with the classic SBR in the presence of an obstacle.

6a. Based on the classic SBR approach, one should consider a reception sphere of appropriate radius around *Rx*, in order to reject rays R_1, R_2, R_4 and R_5, passing at the vicinity of the receiver. On the contrary, by adopting the proposed method, the field's strength at *Rx* is calculated in a straightforward manner, without the need for the consideration of a reception sphere, in order to reject the neighboring rays from the calculations, as demonstrated in Fig. 6b. Given that the "reception-sphere test" is repeated for all points of the study area, this property of the proposed technique reduces the duration of the simulation-predictions, for the same resolution requirements, as will be shown in section IV.

Similarly, when considering a wall in the area of interest, as shown in Fig. 7, the same advantage of the proposed method is preserved. Hence, reflection at point *Rx* will be calculated by ray R_2 as long as *Rx´* is targeted (Fig. 7b).

Theoretically, the use of the reception-sphere test requires that all rays are separated by neighboring ones by constant angles. This however cannot be accomplished in 3D space for any desired resolution. Hence, in the classic SBR technique [4], nearly uniform angular separation is maintained, by adapting solutions from the theory of geodesic domes. Due to the imperfections of the space-division, paths may be duplicated in the receiver [4]. This problem is also overcome in the pro

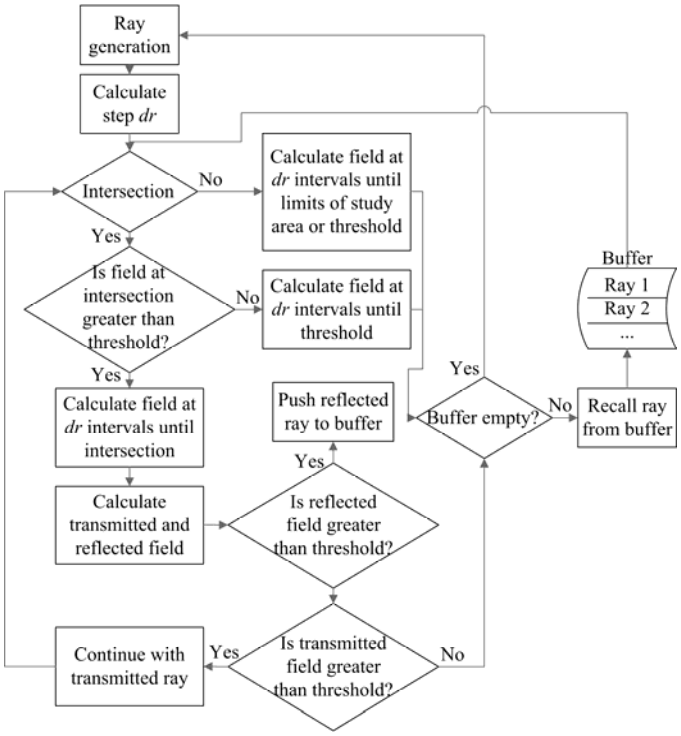

Fig. 8. Flowchart of the algorithm

posed technique.

Finally, the proposed method is straightforward and can be easily implemented in a ray-tracing planning tool.

III. Description of the Algorithm

The flowchart of the algorithm that carries out the calculations in the study area is given in Fig. 8. The calculations for each ray end, either when the signal strength falls below a predefined threshold or when the ray exits the area of interest.

According to E/M field theory, [15]—[16], the polarization state of an E/M wave is altered when reflected in the boundary surface of a lossy medium. The complex reflection coefficients for both perpendicular and parallel (according to the plane of incidence) components of electric field intensity vector $\vec{E}$, are calculated and the polarization effects are taken into account. Moreover, the dielectric constant for all lossy materials is considered complex [17], therefore the phase velocity of a traveling wave inside a thick wall is affected and calculated accordingly. The implemented algorithm for the calculation of all reflection and transmission coefficients is easily adaptable to a set of N intermediate layers inside a wall by using a recursive formula [15]—[16].

Diffraction is calculated by implementing the extension, [18]—[19], to the classic, [20]—[21], UTD dyadic diffraction coefficient for the inclusion of non-perfectly conducting surfaces. Wedges and edges are treated as 2^{ndary} sources of radiation and the same algorithm, represented in Fig. 8, is executed. The gains of the transmitting and the receiving antennas are calculated by implementing the approximation technique presented in [22]. This technique succeeds in well-estimating the

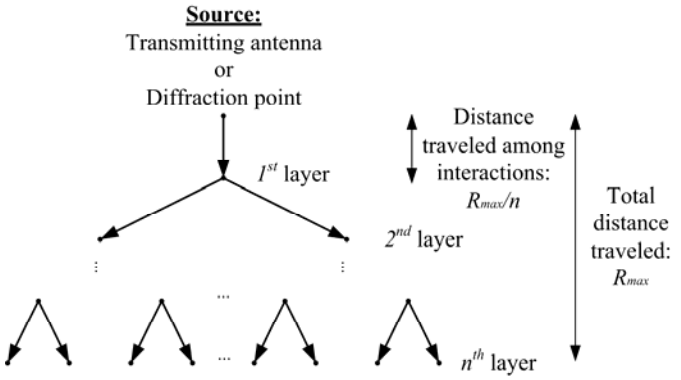

Fig. 9. Ray splitting after successive incidences.

3D radiation pattern of an antenna, by properly combining the two principal cuts.

At each point of the study area, information regarding the power, the direction of arrival, the time of arrival and the polarization state of each ray are stored.

IV. Comparison with the Classic SBR

In order to compare the proposed technique with the classic SBR method, we consider the generation of the same amount of rays; hence, the same resolution is assumed. Moreover, we suppose that the maximum number of interactions of a ray, before it reaches the noise level of the receiver, with the surrounding obstacles of the environment is n, as shown in Fig. 9. The maximum time for the calculation of all possible intersections of a ray generated from the transmitter is common in both techniques and equals $O\left(\left(2^n-1\right)t_{\max}\right)$, where t_{max} is the maximum time to specify an intersection. Similarly, the calculations and storage of the field's values at all points of the study area are common for both techniques.

The only difference, in terms of simulation time, is the reception-sphere test that needs to be performed in the classic SBR approach. In order to estimate the total time saved in the proposed SBR technique, let's assume that the reception-sphere test is repeated for each ray at constant dr intervals and takes time t_{test}. Moreover, let's consider that each ray travels a total distance R_{max}, as shown in Fig. 9, and is subject to n interactions with the surrounding obstacles. Each incidence is assumed to occur at constant distances of R_{max}/n. Hence, after the 1st incidence the generated reflected ray will be subject to $n-1$ interactions traveling a distance of $(n-1)R_{max}/n$. The total time for the reception-sphere test of a source-generated ray is $\left(2^n-1\right)\frac{R_{\max}}{ndr}t_{test}$. Considering N rays generated at each source and M sources, the total time for the reception-sphere tests in the study area is:

$$MN\left(2^n-1\right)\frac{R_{\max}}{ndr}t_{test} \tag{2}$$

In this approach, R_{max} depends on the size of the study area and the dynamic range of the transmit-receive system, dr on

TABLE I
CONSTITUTIVE PARAMETERS OF THE MATERIALS IN SIMULATIONS

Material	Permittivity	Loss tangent
Exterior Concrete Wall [24]	7.0	0.12
Interior Brick Wall [23]	4.26	0.04

TABLE II
RUNNING-TIME FOR DIFFERENT ENVIRONMENTS

Environment	ds	Number of rays	Running-time (s)
Urban	10	186626	220.276
Indoor	2	438914	854.508

the spacing among neighboring study points, t_{test} on the computer's power, M on the environment, n on the E/M characteristics of the materials in the study area, and N on the desired resolution. For example, the proposed technique outperforms the classic SBR by $10^9 t_{test}$, assuming the following typical values: M=5, N=10^5, n=7, R_{max}/dr=100.

A different approach could be followed for the reception-sphere test; e.g. in [3], each "ray segment is tested to see if it can be considered to have reached specified receiving locations in the same room". In any case, the proposed SBR method is straightforward and guarantees faster predictions for the same resolution requirements.

V. RESULTS

Some typical results of the received signal strength for both outdoor and indoor environments are given in Figs. 10—11, where larger power levels are represented with darker variations of gray. The view for all extracted plots is handled by utilizing the standard OpenGL graphics acceleration routings that allow fast redrawing and changing of viewpoints. The constitutive parameters of the materials considered for the simulations are summarized in table I, [23]—[24].

In Fig. 10, a typical urban layout was considered. The antenna was placed well below rooftop level at 12m height, transmitting 1W at 1800MHz. A directional antenna manufactured by Kathrein with 16.5 dBi gain (model 742241), tilted 6º downwards, was considered. For the values shown in Fig. 10, a theoretical isotropic receiving antenna at 2m height was considered. The average received power level was calculated using the following equation assuming that the phases of the multipath components were random variables uniformly distributed in (0,2π).

$$\hat{P} = \frac{\lambda^2}{4\pi}\frac{1}{2\eta}\sum_i G_R(\theta_i,\phi_i)E_i^2 \qquad (3)$$

where λ is the wavelength, η the free space impedance, and E_i and $G_R(\theta_i,\phi_i)$ the intensity of the electric field of the specific component and receiver's gain value at the angles (θ_i,φ_i) respectively.

A single-floor building was considered in the 2nd scenario, represented in Fig. 11. This time the antenna was set at 2.9m height and the receiver at 1m height.

The running times of the corresponding plots of Figs. 10—11 are given in table II. The simulations were carried out in a Pentium M 1.5GHz processor. Different selection of the spacing of the "Study set" was made, based on the desired resolution in the two different cases. Hence, for the outdoor environment, 10m spacing was considered adequate, whereas 2m spacing was selected for the indoor case. The simulation lasted only 3′40′′ for the urban case and 14′14′′ for the indoor scenario, due to the greater number of launched rays. In any case small prediction-times were maintained. More accurate results -better resolution- can be derived at the expense of worse running-times.

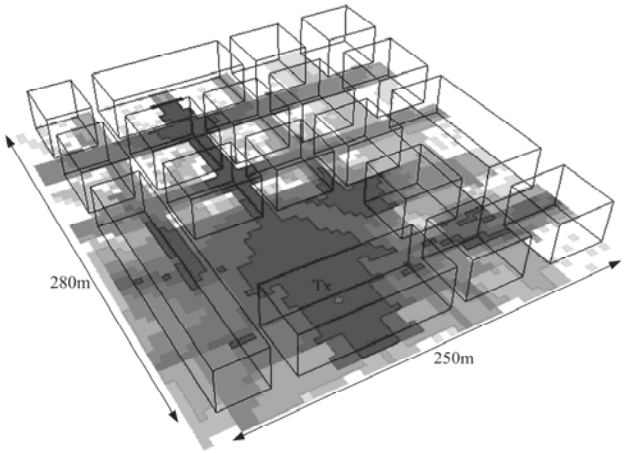

Fig. 10. Received power level for a typical urban small area configuration.

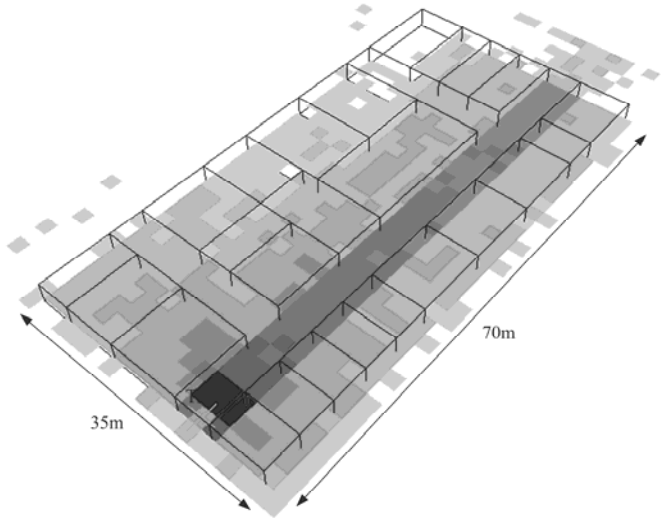

Fig. 11. Received power level for an indoor environment.

The total time saved in the urban case is approximately $3.55\times10^9\times t_{test}$, substituting M=21, N=186626, n=7, and R_{max}/dr=50 in (2). It is hard to estimate t_{test}, since it depends not only on the ability of a system to compute floating point operations (measured in Mflops-million operations per second), but also on the status of the system at simulation and the compiler. Hence, the actual time for performing an operation

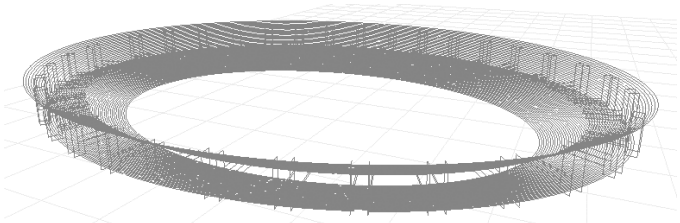

Fig. 12. Model of the Olympic stadium as used in the simulations.

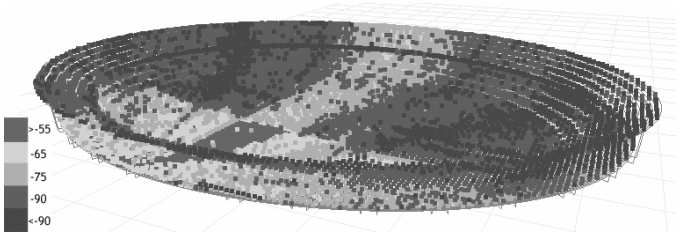

Fig. 13. Received power level (dBm) results obtained with proposed SBR technique.

in C++, e.g. a multiplication, is usually much greater than the computational capabilities of the system. In order to acquire a rough estimation of t_{test}, in the same conditions where the above results were obtained, a short code was executed, that performs the reception-sphere test with 3 rays, and t_{test} was measured equal to 1.17×10^{-6}s. Therefore, in the urban case the total estimated time saved would be 1h and 10 minutes. Obviously, this is an overestimation of the running-time saved, since we have supposed that all generated rays (and their children) are subject to the 7-layer incidence-model, suggested in Fig. 9, which is not the case of Fig. 10. However, definitely, several minutes were saved. Following similar approximation, the total time saved in the indoor case is estimated 12 minutes (and is considered closer to the actual).

The proposed algorithm has been successfully used to provide propagation-predictions, for the design of the GSM cellular network inside the Olympic Stadium for the Olympic Games of 2004. The model of the stadium and a typical result are shown in Figs. 12 and 13 respectively.

VI. Conclusions

In this paper, a new SBR technique has been put forward. The proposed technique is appropriate for both indoor and outdoor applications, demonstrating high accuracy at small running times.

It was shown that the proposed method is considerably faster than the classic SBR techniques for the same resolution requirements. This is accomplished by implementing a shooting concept that is oriented towards a straightforward calculation of the field's values at the points of interest, rather than attempting to divide space in almost equal solid angles. Hence, the proposed approach suits better the typical cubic calculations' grid, than the classic approaches that would match a spherical study grid.

References

[1] J. W. McKown and R. L. Hamilton Jr., "Ray tracing as design tool for radio networks," *IEEE Network, The magazine of computer communications,* pp. 27-30, Nov. 1991.

[2] M. C. Lawton and J. P. McGeehan, "The application of a deterministic ray launching algorithm for the prediction of radio channel characteristics in small-cell environments," *IEEE Trans. Veh. Technol.*, vol. 43, no. 4, pp. 955—969, Nov. 1994.

[3] W. Hocharenko, H. L. Bertoni, J. L. Dailing, J. Qian, and H. D. Yee, "Mechanisms governing UHF propagation on single floors in modern office buildings," *IEEE Trans. Veh. Technol.*, vol. 41, no. 4, pp. 496—504, Nov. 1992.

[4] S. Y. Seidel and T. S. Rappaport, "Site-specific propagation prediction for wireless in-building personal communication system design," *IEEE Trans. Veh. Technol.*, vol. 43, no. 4, pp. 879—891, Nov. 1994.

[5] C.-F. Yang, B.-C. Wu, and C.-J. Ko, "A ray-tracing method for modeling indoor wave propagation and penetration," *IEEE Trans. Antennas Propagat.*, vol. 46, no. 6, pp. 907—919, June1998.

[6] G. Liang and H. L. Bertoni, "A new approach to 3-D ray tracing for propagation prediction in cities," *IEEE Trans. Antennas Propagat.*, vol. 46, no. 6, pp. 853—863, June 1998.

[7] W. M. O' Brien, E. M. Kenny, and P. J. Cullen, "An efficient implementation of a three-dimensional microcell propagation tool for indoor and outdoor urban environments," *IEEE Trans. Veh. Technol.*, vol. 49, no. 2, pp. 622–630 March 2000.

[8] G. E. Athanasiadou and A. R. Nix, "A novel 3-D indoor ray-tracing propagation model: the path generator and evaluation of narrow-band and wide-band predictions," *IEEE Trans. Veh. Technol.*, vol. 49, no. 4, pp. 1152—1168, July 2000.

[9] J.-P. Rossi and Y. Gabillet, "A mixed ray launching/tracing method for full 3-D UHF propagation modeling and comparison with wide-band measurements," *IEEE Trans. Antennas Propagat.*, vol. 50, no. 4, pp. 517—523, April 2002.

[10] S.-C. Kim, B. J. Guarino Jr., T. M. Willis III, V. Erceg, S. J. Fortune, R. A. Valenzuela, L. W. Thomas, J. Ling, and J. D. Moore, "Radio propagation measurements and prediction using three-dimensional ray tracing in urban environments at 908 MHz and 1.9 GHz," *IEEE Trans. Veh. Technol.*, vol. 48, no. 3, pp. 931—946, May 1999.

[11] Z. Chen, H. L. Bertoni, and A.Delis, "Progressive and approximate techniques in ray-tracing-based radio wave propagation prediction models," *IEEE Trans. Antennas Propagat.*, vol. 52, no. 1, pp. 240—251, Jan. 2004.

[12] M. F. Catedra and J. Perez-Arriaga, *Cell Planning for Wireless Communications*. Boston-London: Artech House, 1999.

[13] S. R. Saunders, *Antennas and Propagation for Wireless Communication Systems*, John Wiley & Sons, 1999.

[14] T. K. Sarkar, Z. Ji, K. Kim, A. Medour, and M. Salazar-Palma, "A survey of various propagation models for mobile communication," *IEEE Antennas Propagat. Mag.*, Vol. 45, No. 3, pp. 51—82, June 2003

[15] C. A. Balanis, *Advanced Engineering Electromagnetics*. Wiley, 1989.

[16] D. Paris, and K. Hurd, *Basic Electromagnetic Theory*. McGraw-Hill, 1969.

[17] A. Von Hippel, *Dielectric Materials and Applications*. Boston: Artech House, 1995.

[18] W. D. Burnside and K. W. Burgener, "High frequency scattering by a thin lossless dielectric slab," *IEEE Trans. Antennas Propagat.*, vol. 31, no. 1, pp. 104-110, Jan. 1983.

[19] R. J. Luebbers, "Finite conductivity uniform GTD versus knife edge diffraction in prediction of propagation path loss," *IEEE Trans. Antennas Propagat.*, vol. 32, no. 1, pp. 70-76, Jan. 1984.

[20] J. B. Keller, "Geometrical theory of diffraction," *J. Opt. Soc. Amer.*, vol. 52, no. 2, pp 116-130, Feb. 1962.

[21] R. G. Kouyoumjian and P. H. Pathak, "A uniform geometrical theory of diffraction for an edge in a perfectly conducting surface," *Proc. IEEE*, vol. 62, no. 11, pp. 1448-1461, Nov. 1974.

[22] T. G. Vasiliadis, A. G. Dimitriou, and G. D. Sergiadis, "A novel technique for the approximation of 3D antenna radiation patterns," *IEEE Trans. Antennas Propagat.*, to be published.

[23] S. Stavrou, and S. R. Saunders, "Review of constitutive parameters of materials," *in 12th ICAP*, vol. 1, pp. 211—215, April 2003.

[24] ITU-R, Recommendation ITU-R P. 1238-2, 2001